Inorg. Chem. **2005**, *44*, 7678−7685

Inorganic Chemistry
Article

$[Ru(phen)_2(PHEHAT)]^{2+}$ and $[Ru(phen)_2(HATPHE)]^{2+}$: Two Ruthenium(II) Complexes with the Same Ligands but Different Photophysics and Spectroelectrochemistry

Arnaud Boisdenghien, Cécile Moucheron, and Andrée Kirsch-De Mesmaeker*

Université Libre de Bruxelles, Chimie Organique et Photochimie, CP 160/08,
50 avenue F.D. Roosevelt, B-1050 Bruxelles, Belgium

Received August 2, 2005

The properties of two mononuclear Ru(II) complexes formed with the extended planar ligand PHEHAT depend drastically on the chelation site by the metallic ion. When the chelation takes place on the HAT site of the ligand (case of the novel complex $[Ru(phen)_2(HATPHE)]^{2+}$), the emission behavior is quite similar to that of $[Ru(phen)_2(HAT)]^{2+}$. In contrast, when the chelation is on the phen motif of the ligand (case of $[Ru(phen)_2(PHEHAT)]^{2+}$), the spectroscopic (absorption and emission) and electrochemical data for the complex do not obey the linear spectroelectrochemical correlation and the emission behavior is comparable to that of the extensively studied dppz complex ($[Ru(phen/bpy)_2(dppz)]^{2+}$). Thus, for $[Ru(phen)_2(PHEHAT)]^{2+}$, the emission lifetimes and intensities as a function of temperature exhibit a maximum for nitrile solvents. However, in contrast to the dppz case, at least three different states (two emitting and one dark) participate in the deactivation with different contributions depending on the temperature. These different contributions explain the observed maximum. Moreover, the fact that the solvent is liquid or frozen also influences the nature of the luminescent species.

Introduction

The well-known $[Ru(phen/bpy)_2(dppz)]^{2+}$ (phen = 1,10-phenanthroline, bpy = 2,2′-bipyridine, dppz = dipyrido[3,2-*a*:2′,3′-*c*]phenazine) complex has been exploited in several works as an intercalating agent toward nucleic acids.[1−4] The increasing interest for these complexes may be attributed mainly to the fact that they do not emit in water but their luminescence is switched on by addition of DNA. Several experimental[5,6] and theoretical[7,8] studies have been carried out to clarify these intriguing properties of light-switching. Brennaman et al.[6,9] measured the emission lifetime of $[Ru(bpy)_2(dppz)]^{2+}$ [9] in solvents such as acetonitrile or butyronitrile and in different alcohols as a function of temperature. They observed that a decrease of temperature produces, as expected, an increase in the excited-state lifetime, which originates from a drop of thermal population of the nonemitting ^{3}MC (metal centered) state from the ^{3}MLCT (metal to ligand charge transfer) state. However from a given temperature, which depends on the solvent, this lifetime reaches a maximum and starts decreasing at lower temperatures. They have attributed this “abnormal” decrease of lifetime to the existence of a dark CT (charge transfer) state, whose population increases by lowering the temperature. Therefore, the authors proposed the following model. A bright (B, luminescent) ^{3}MLCT state is in thermodynamic equilibrium with a dark (D, nonluminescent) CT state. The bright state is entropically driven whereas the dark state is energetically driven, thus lower in energy than the luminescent ^{3}MLCT state.

---

* To whom correspondence should be addressed. E-mail: akirsch@ulb.ac.be.

(1) Jenkins, Y.; Friedman, A. E.; Turro, N. J.; Barton, J. K. *Biochemistry* **1992**, *31*, 10809−10816.
(2) Lincoln, P.; Broo, A.; Norden, B. *J. Am. Chem. Soc.* **1996**, *118*, 2644−2653.
(3) Coates, C. G.; McGarvey, J. J.; Callaghan, P. L.; Coletti, M.; Hamilton, J. G. *J. Phys. Chem. B* **2001**, *105*, 730−735.
(4) Friedman, A. E.; Chambron, J. C.; Sauvage, J. P.; Turro, N. J.; Barton, J. K. *J. Am. Chem. Soc.* **1990**, *112*, 4960−4962.
(5) Olson, E. J. C.; Hu, D.; Hörmann, A.; Jonkman, A. M.; Arkin, M. R.; Stemp, E. D. A.; Barton, J. K.; Barbara, P. F. *J. Am. Chem. Soc.* **1997**, *119*, 11458−11467.
(6) Brennaman, M. K.; Alstrum-Acevedo, J. H.; Fleming, C. N.; Jang, P.; Meyer, T. J.; Papanikolas, J. M. *J. Am. Chem. Soc.* **2002**, *124*, 15094−15098.
(7) Pourtois, G.; Beljonne, D.; Moucheron, C.; Schumm, S.; Kirsch-De Mesmaeker, A.; Lazzaroni, R.; Bredas, J. L. *J. Am. Chem. Soc.* **2004**, *126*, 683−692.
(8) Batista, E. R.; Martin, R. L. *J. Phys. Chem. A* **2005**, *109*, 3128−3133.
(9) Brennaman, M. K.; Meyer, T. J.; Papanikolas, J. M. *J. Phys. Chem. A* **2004**, *108*, 9938−9944.

10.1021/ic051306f CCC: $30.25

$$B \rightleftharpoons D \qquad K = [D]/[B] = \exp[-(\Delta G^\circ/RT)] = \exp[-(\Delta H^\circ - T\Delta S^\circ)/RT]$$

Formation of D is accompanied by a decrease of entropy ($\Delta S^\circ < 0$), but it is favored enthalpically ($\Delta H^\circ < 0$). The decrease of entropy by formation of the lowest energy state is proposed to be attributed to a localization of the excited electron no longer on the bpy moiety (as in the B state) but on the pyrazine moiety of the dppz ligand. In the domain of temperature lower than the temperature corresponding to the maximum lifetime, a temperature domain in which the term $-T\Delta S^\circ$ plays a negligible role, the population of the D state increases.

On the other hand, on the basis of theoretical studies,[7,8] a dppz-centered $^3\pi-\pi^*$ excited state has been calculated as the lowest state depending on the method of calculation and medium effect.[8] This $^3\pi-\pi^*$ state has been suggested as corresponding to this dark state.[7]

For hydroxylic solvents such as water and alcohols, a slightly different model has been proposed by other authors[10,11] to take into account the luminescent behavior of $[Ru(phen)_2(dppz)]^{2+}$. From detailed spectroscopic and dynamic studies, it is concluded that, in addition to the luminescent ^{3}MLCT state in which the charge has been transferred from the Ru to the dppz ligand, two other states participate in the photophysical behavior: a second emitting state lower in energy with one H-bond between the solvent and the first nitrogen of the dppz pyrazine ring and a third nonemitting state, still lower in energy, with two H-bonds with the two dppz nitrogens. These three states are in equilibrium.

These results for hydroxylic and for nitrile solvents illustrate the complexity of the luminescence behavior of the dppz Ru complexes.

In our laboratory, Ru compounds containing another planar DNA intercalating ligand, PHEHAT (PHEHAT = 1,10-phenanthrolino[5,6-*b*]1,4,5,8,9,12-hexaazatriphenylene) (Chart 1), with two possible chelation sites, have been prepared and studied.

Chart 1. Two Chelation Sites of the PHEHAT/HATPHE Ligand[a]

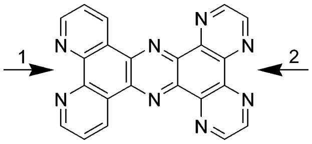

[a] PHEHAT = complexation at 1; HATPHE = complexation at 2.

For example, complexes such as $[Ru(phen)_2(PHEHAT)]^{2+}$ [12] and $[Ru(TAP)_2(PHEHAT)]^{2+}$ (TAP = 1,4,5,8-tetraazaphenanthrene)[13] were examined in the absence and presence of DNA. In both compounds, the metal center is chelated to the PHEHAT via the phen motif of the ligand. Between these two PHEHAT complexes, there are tremendous differences in their behavior under illumination. The TAP-containing complex is able to abstract an electron from the guanine bases of DNA, and moreover, it does luminesce ($\tau = 842$ ns; $\lambda_{max} = 636$ nm, under air) in water and obeys the spectroelectrochemical correlation as found for most complexes.[14] In contrast the phen-containing complex behaves very much like $[Ru(phen)_2(dppz)]^{2+}$ or $[Ru(bpy)_2(dppz)]^{2+}$; thus, it does not luminesce in water but it emits in organic solvents and in DNA containing aqueous solutions. In the case of the TAP compound, the lowest ^{3}MLCT state corresponds to a charge transfer to the TAP ligand (thus ^{3}MLCT Ru−TAP) so that the luminescence is governed by this luminophore, the same as in $[Ru(TAP)_3]^{2+}$ for example.[15] In the case of the phen compound, the luminescence is controlled by a ^{3}MLCT state Ru−PHEHAT which seems to exhibit properties similar to those of the ^{3}MLCT state of the dppz complexes as described above.

In this work, to shed light on this peculiar behavior of $[Ru(phen)_2(PHEHAT)]^{2+}$, in addition to its photophysical study by comparison with the dppz compounds, we have prepared and examined another complex, $[Ru(phen)_2(HATPHE)]^{2+}$, in which the PHEHAT ligand is chelated to the Ru(II) center via the HAT motif of the ligand. The characteristics of this new complex are discussed and compared to those of $[Ru(phen)_2(PHEHAT)]^{2+}$. To specify the site of chelation of the planar ligand in the complex (Chart 1), it will be called PHEHAT when the phen motif is chelated and HATPHE when the HAT motif is chelated.

Interestingly, we show also that the spectroelectrochemical properties of the two compounds ($[Ru(phen)_2(PHEHAT)]^{2+}$ and $[Ru(phen)_2(HATPHE)]^{2+}$) are completely different. For $[Ru(phen)_2(PHEHAT)]^{2+}$, the results are also discussed on the basis of the data published for $[Ru(bpy)_2(dppz)]^{2+}$ and its derivatives.[6,9,16]

Experimental Section

Instrumentation. The proton NMR data were obtained on a Bruker Avance-300 instrument. The ESMS (electrospray mass spectrometry) analyses were carried out on a VG Bio-QUAD mass spectrometer at the University Louis Pasteur (Strasbourg, France). The absorption spectra were recorded on a Perkin-Elmer Lambda 40 UV/vis spectrophotometer, and the emission data, with a Shimadzu RF-5001 PC spectrofluorometer equipped with a xenon lamp (250 W) as exciting source and a Hamamatsu R-928 red-sensitive photomultiplier tube for the detection. Cyclic voltammetry was carried out on a carbon disk working electrode (approximate area = 3 mm^2), in dried acetonitrile with tetrabutylammonium perchlorate as supporting electrolyte. The counter electrode was a platinum wire, and the reference electrode a saturated calomel electrode (SCE). All the measurements were performed in a one-compartment cell. The emission lifetimes were measured by using the single-photon counting technique (SPC) with an Edimburgh Instruments FL900 spectrometer (Edinburgh, U.K.) equipped with

---

(10) Olofsson, J.; Onfelt, B.; Lincoln, P. *J. Phys. Chem. A* **2004**, *108*, 4391−4398.

(11) Olofsson, J.; Wilhelmsson, L. M.; Lincoln, P. *J. Am. Chem. Soc.* **2004**, *126*, 15458−15465.

(12) Moucheron, C.; Kirsch-De Mesmaeker, A.; Choua, S. *Inorg. Chem.* **1997**, *36*, 584−592.

(13) Moucheron, C.; Kirsch-De Mesmaeker, A. *J. Phys. Org. Chem.* **1998**, *11*, 577−583.

(14) Moucheron, C.; Kirsch-De Mesmaeker, A.; Kelly, J. M. *J. Photochem. Photobiol., B* **1997**, *40*, 91−106.

(15) Masschelein, A.; Jacquet, L.; Kirsch-De Mesmaeker, A.; Nasielski, J. *Inorg. Chem.* **1990**, *29*, 855−860.

(16) Onfelt, B.; Olofsson, J.; Lincoln, P.; Nordén, B. *J. Phys. Chem. A* **2003**, *107*, 1000−1009.

a nitrogen-filled discharge lamp and a peltier-cooled Hamamatsu R955s photomultiplier tube. The emission decays were analyzed with the Edinburgh Instruments software (version 3.0), based on nonlinear least-squares regressions using Marquardt algorithms. Low-temperature emission lifetimes were obtained using an Oxford instruments DN 1704 nitrogen cryostat controlled by an Oxford Intelligent Temperature Controller (ITC4) instrument. The transient emissions were detected by a modified Applied Photophysics laser kinetic spectrometer equipped with a monochromator (Applied Photophysics f/3.4) and a red-sensitive Hamamatsu R928 photomultiplier tube connected to an oscilloscope HP 5248. A harmonic wavelength of the pulsed Nd:YAG laser was used as the excitation source (Continuum NY 61-10, excitation wavelength 355 nm; 6 mJ/pulse). The data were transferred to a PC to determine the lifetimes.

Chemicals. The solvents used for the photophysical measurements were of spectroscopic grade. Acetonitrile for cyclic voltammetry was distilled twice over P_2O_5 and once over CaH_2. The starting compounds ($RuCl_3$; 1,10-phenanthroline; 1,3,5-trichlorobenzene; glyoxal) were obtained from Sigma-Aldrich, and water was purified with a Millipore Milli-Q system.

Syntheses. $[Ru(phen)_2Cl_2]$ (bis(1,10-phenanthroline)dichlororuthenium(II)), diamino-TAP (9,10-diamino-1,4,5,8-tetraazaphenanthrene), phendione (1,10-phenanthrolino-5,6-dione), and $[Ru(phen)_2(PHEHAT)]^{2+}$ were prepared by following procedures described in the literature.[12,17,18]

Synthesis of $[Ru(phen)_2(diamino\text{-}TAP)]^{2+}$. The reaction of 130 mg of diamino-TAP (0.612 mmol) with 300 mg of $[Ru(phen)_2Cl_2]$ (0.563 mmol) was performed in 20 mL of a mixture ethanol−water [50:50 (v/v)] under reflux during 6 h. After being cooled at room temperature, the product was precipitated with a few drops of a saturated hexafluorophosphate ammonium aqueous solution. The complex $[Ru(phen)_2(diamino\text{-}TAP)]^{2+}$ (bis(1,10-phenanthroline)-(9,10-diamino-1,4,5,8-tetraazaphenanthrene)ruthenium(II)) was isolated by centrifugation and washed several times with water, ethanol, and ether. It was purified by silica gel preparative layer chromatography using CH_3CN-H_2O-aqueous solution saturated in NH_4Cl [5:5:1 (v/v/v)]. A 250 mg (0.259 mmol) amount of the desired complex was obtained, corresponding to a total yield of 46%. The complex $[Ru(phen)_2(diamino\text{-}TAP)]^{2+}$ was characterized by proton NMR spectroscopy. ^1H NMR (300 MHz, CD_3CN): δ 8.65 (d, 2H, $J = 2.8$ Hz, $H_\delta{}^{dT}$), 8.63 (dd, 2H, $J = 8.3$, 1.2 Hz, $H_4{}^P$), 8.62 (dd, 2H, $J = 8.3$, 1.2 Hz, $H_7{}^P$), 8.25 (s, 4H, $H_{5,6}{}^P$), 8.07 (dd, 2H, $J = 5.2$ 1.2 Hz, $H_2{}^P$), 7.99 (dd, 2H, $J = 5.3$, 1.2 Hz, $H_9{}^P$), 7.82 (d, 2H, $J = 2.8$ Hz, $H_\epsilon{}^{dT}$), 7.65 (dd, 2H, $J = 5.2$, 8.3 Hz, $H_3{}^P$), 7.63 (dd, 2H, $J = 8.3$, 5.3 Hz, $H_8{}^P$), 5.35 (s, 4H, $H_{NH}2^{dT}$).

Synthesis of $[Ru(phen)_2(HATPHE)]^{2+}$. A 6.01 mg (0.0286 mmol) amount of phendione was condensed with 25 mg (0.0260 mmol) of $[Ru(phen)_2(diamino\text{-}TAP)]^{2+}$ in 8 mL of a mixture ethanol−acetic acid−water [10:4:1 (v/v/v)]. The reaction mixture was kept refluxing for 1 h. The $[Ru(phen)_2(HATPHE)]^{2+}$ (bis(1,10-phenanthroline)(1,10-phenanthrolino[5,6-*b*]1,4,5,8,9,12-hexaazatriphenylene)ruthenium(II)) was precipitated with a few drops of a saturated hexafluorophosphate ammonium aqueous solution and washed several times with water, ethanol, and ether. After purification by preparative layers chromatography on silica gel {CH_3CN-H_2O-aqueous solution saturated in NH_4Cl [5:5:1 (v/v/v)]}, 15 mg (0.0176 mmol) of the desired complex was obtained (67% yield). The complex was characterized by proton NMR spectroscopy and by electrospray mass spectrometry. ^1H NMR (300 MHz, CD_3CN): δ 9.72 (dd, 2H, $H_\gamma{}^{HP}$), 9.12 (dd, 2H, $H_\alpha{}^{HP}$), 9.08 (d, 2H, $J = 2.9$ Hz, $H_\delta{}^{HP}$) 8.70 (dd, 2H, $J = 1.1$ Hz, $H_7{}^P$), 8.68 (dd, 2H, $J = 1.1$ Hz, $H_4{}^P$), 8.40 (dd, 2H, $J = 5.2$, Hz, $H_2{}^P$), 8.34 (d, 2H, $H_\epsilon{}^{HP}$), 8.31 (s, 4H, $H_{5,6}{}^P$), 8.04 (dd, 2H, $J = 5.2$ Hz, $H_9{}^P$), 7.98 (dd, 2H, $J = 4.5$, 8.2 Hz, $H_\beta{}^{HP}$), 7.71 (dd, 2H, $J = 8.3$ Hz, $H_8{}^P$), 7.70 (dd, 2H, $J = 8.2$ Hz, $H_3{}^P$).

Scheme 1. Synthesis of $[Ru(phen)_2((hatphe)]^{2+}$

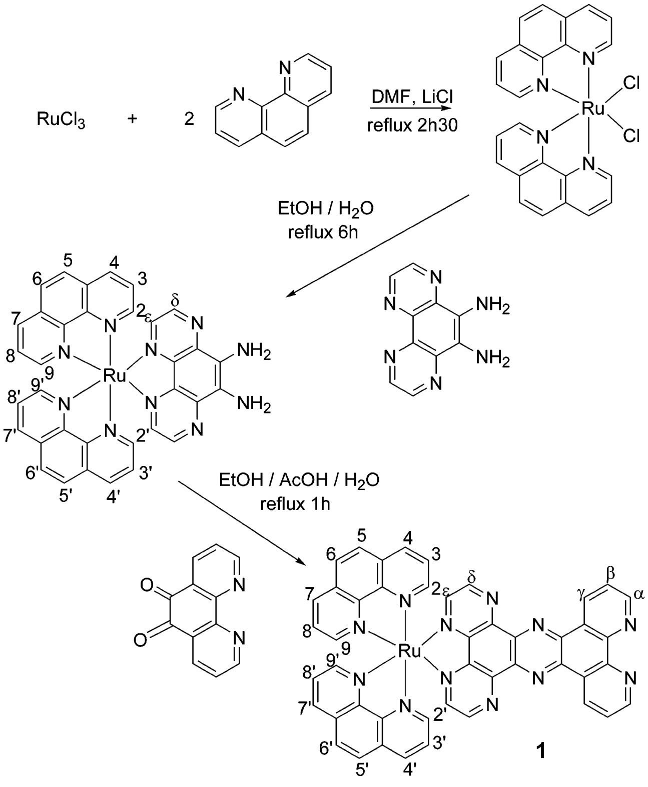

ESMS *m*/*z* (intensity) {calcd}: 993.4 (5%) {992.8} ($[M - PF_6]^+$) and 423.5 (100%) {423.9} ($[M - 2PF_6]^{2+}$) with M = 1137.68 g/mol. Elemental analysis: found (calcd): C: 48.59 (48.56), H: 2.18 (2.30), N: 14.02 (14.77).

Results

The new complex $[Ru(phen)_2(HATPHE)]^{2+}$ has been synthesized according to the procedure described in Scheme 1. In a first step, the precursor $[Ru(phen)_2Cl_2]$ reacts with diamino-TAP to yield $[Ru(phen)_2(diamino\text{-}TAP)]^{2+}$ (46% yield). In a second step, this complex is condensed with 1,10-phenanthroline-5,6-dione and furnishes $[Ru(phen)_2(HATPHE)]^{2+}$ with 67% yield.

The HATPHE complex is characterized by ES mass spectroscopy and NMR. The chemical shifts of the protons H_α, H_β, and H_γ depend on the concentration of the complex, which indicates a π-stacking interaction between the extended aromatic HATPHE ligands. The shielding of the two protons ϵ indicates chelation on the adjacent nitrogens. The resonance of the γ protons at low field proves the formation of the extended planar aromatic heptacycle.

Electrochemical Data. The redox potentials in acetonitrile for the HATPHE, PHEHAT, and HAT complexes (first oxidation and first reduction wave) are reported in Table 1

---

(17) Sullivan, B. P.; Salmon, D. J.; Meyer, T. J. *Inorg. Chem.* **1978**, *17*, 3334−3341.

(18) Hartshorn, R. M.; Barton, J. K. *J. Am. Chem. Soc.* **1992**, *114*, 5919−5925.

Table 1. Redox Potentials for the Ruthenium(II) Complexes in MeCN[a]

complex	E_{red}/V	E_{ox}/V
HAT	-1.33	
PHEHAT	-1.10	
dppz[b,19]	-1.18^{d}	
$[Ru(phen)_3]^{2+}$[20]	-1.41^{r}	$+1.40^{r}$
$[Ru(phen)_2(HAT)]^{2+}$[21]	-0.86^{r}	$+1.53^{r}$
$[Ru(phen)_2(dppz)]^{2+}$[22]	-1.00^{r}	$+1.30^{r}$
$[Ru(phen)_2(PHEHAT)]^{2+}$[12]	$-0.95 \rightarrow -1.05^{c,d}$	$+1.35^{r}$
$[Ru(phen)_2(HATPHE)]^{2+}$	-0.83^{r}	$+1.56^{r}$

[a] The redox potentials (V/SCE) were determined by cyclic voltammetry in acetonitrile (for complexes) and in DMF (for the ligands) (supporting electrolyte: $(But)_4N^+ClO_4^-$, 10^{-1} M) with a glassy carbon electrode as working electrode. r = reversible. [b] Mercury working electrode. [c] For unclear reasons, the reduction potential value was not reproducible and varied between −0.95 and −1.05 V. [d] The values reported in the table originate from this work for a better comparison with the new data.

Table 2. Absorption Data for the Ruthenium(II) Complexes[a]

	λ_{max}/nm ($\epsilon/10^{-4}$ M^{-1} cm^{-1})	
complex	H_2O	MeCN
$[Ru(phen)_3]^{2+}$	421, 447 (1.90)[23]	262 (12.5), 446 (1.99)[24]
$[Ru(phen)_2(HAT)]^{2+}$[21]	262, 430 (1.44), 494 sh	262, 420, 480 sh
$[Ru(phen)_2(PHEHAT)]^{2+}$	264, 276 sh, 312 sh, 356, 374, 440 (2.27)	264, 278 sh, 312 sh, 354 sh, 370, 438
$[Ru(phen)_2(HATPHE)]^{2+}$	258, 290, 316, 364, 382, 451 (1.47), 490 sh	260, 288 sh, 316, 364, 382, 428, 478 sh

[a] Error on ϵ: ~10%. sh = shoulder.

together with the reduction potentials of the free ligands HAT, PHEHAT, and dppz in DMF (HAT = 1,4,5,8,9,12-hexaazatriphenylene). The oxidation potential values, which correspond to the abstraction of one electron from the Ru(II) center, are more positive (by ~0.2 V) for $[Ru(phen)_2(HATPHE)]^{2+}$ and $[Ru(phen)_2(HAT)]^{2+}$ than for $[Ru(phen)_2(PHEHAT)]^{2+}$. The first reduction potentials on the other hand, which correspond to the addition of the first electron to the planar extended ligand, are less negative for $[Ru(phen)_2(HATPHE)]^{2+}$ and $[Ru(phen)_2(HAT)]^{2+}$ than for $[Ru(phen)_2(PHEHAT)]^{2+}$.

Absorption and Emission Data. The absorption data in water (and acetonitrile) for $[Ru(phen)_2(HATPHE)]^{2+}$ and the reference complexes are gathered in Table 2. The LC (ligand centered) bands at 364 (364) and 382 (382) nm in $[Ru(phen)_2(HATPHE)]^{2+}$ can be compared to those at 356 (354) and 374 (370) nm in $[Ru(phen)_2(PHEHAT)]^{2+}$ and are attributed to the $\pi-\pi^*$ absorption of the planar extended ligand PHEHAT present in both complexes. The λ_{max} of the shoulder of the MLCT band in $[Ru(phen)_2(HATPHE)]^{2+}$ of 490 (478) nm is very close to that of the reference complex $[Ru(phen)_2(HAT)]^{2+}$ of 494 (480) nm. These data suggest that in absorption the novel HATPHE complex does essentially behave like $[Ru(phen)_2(HAT)]^{2+}$ in water and acetonitrile. Moreover, the most bathochromic MLCT bands of $[Ru(phen)_2(HATPHE)]^{2+}$ (451 nm, shoulder at 490 nm in water, 428 nm, shoulder at 478 nm in MeCN) are red shifted compared to those of $[Ru(phen)_2(PHEHAT)]^{2+}$ (440 nm in water, 438 nm in MeCN).

The emission data are collected in Table 3. The emission maximum of $[Ru(phen)_2(HATPHE)]^{2+}$ in water and acetonitrile is about the same as that of $[Ru(phen)_2(HAT)]^{2+}$. On the other hand, the emission is red shifted (by 0.11 eV from 662 to 692 nm) as compared to that of $[Ru(phen)_2(PHEHAT)]^{2+}$ in MeCN. No comparison is of course possible in water since the PHEHAT complex does not emit in that solvent, which constitutes also an important difference with the HATPHE complex. The luminescence lifetimes and the corresponding radiative (k_r) and nonradiative (k_{nr}) rate constants in water and acetonitrile, as determined from the quantum yields of luminescence (Table 3), have been determined. The k_r and k_{nr} values for $[Ru(phen)_2(HATPHE)]^{2+}$ and $[Ru(phen)_2(HAT)]^{2+}$ are rather close and different from the value of the PHEHAT complex. This suggests similar photophysical properties for $[Ru(phen)_2(HATPHE)]^{2+}$ and $[Ru(phen)_2(HAT)]^{2+}$. The emission lifetimes of $[Ru(phen)_2(HATPHE)]^{2+}$, $[Ru(phen)_2HAT]^{2+}$, and $[Ru(phen)_2(PHEHAT)]^{2+}$ were also measured as a function of temperature in butyronitrile (Figure 1).

Whereas $[Ru(phen)_2(HAT)]^{2+}$ and $[Ru(phen)_2(HATPHE)]^{2+}$ behave normally and exhibit a monotonic increase of emission lifetime by decreasing the temperature, the PHEHAT complex behaves qualitatively like $[Ru(bpy)_2(dppz)]^{2+}$;[6] i.e., there is a maximum in emission lifetime. The steady-state emissions (integrated emission spectra) were also examined as a function of temperature for three different solvents, butyronitrile, propionitrile, and acetonitrile (Figure 2).

A maximum appears in the three curves and, for butyronitrile, approximately in the same temperature range as for the emission lifetimes. The value of T_{max} increases from butyronitrile to propionitrile to acetonitrile. In parallel with these lifetimes and intensities measurements, the λ_{max} of emission of the HATPHE, HAT, and PHEHAT complexes have also been determined in butyronitrile as a function of temperature; the data for $[Ru(phen)_3]^{2+}$ have been added for comparison (Figure 3).

Interestingly, whereas the λ_{max} values for the HAT and HATPHE complexes remain quasi constant with temperature at around 690−710 nm, the λ_{max} of the PHEHAT compound varies from 630 to 720 nm in the temperature range 340−220 K. These emission data suggest that there is only one emitting species for the HAT and HATPHE complexes in the whole investigated temperature range. In contrast, at least two emitters participate to the luminescence in the case of the PHEHAT complex: one in the higher temperature domain, which seems to emit at a λ_{max} approaching that of

---

(19) Chambron, J.-C.; Sauvage, J.-P.; Amouyal, E.; Koffi, P. *New J. Chem.* **1985**, *9*, 527−529.
(20) Tokel-Takvoryan, N. E.; Hemingway, R. E.; Bard, A. J. *J. Am. Chem. Soc.* **1973**, *95*, 6582−6589.
(21) Jacquet, L.; Kirsch-De Mesmaeker, A. *J. Chem. Soc., Faraday Trans.* **1992**, *88*, 2471−2480.
(22) Ortmans, I.; Elias, B.; Kelly, J. K.; Moucheron, C.; Kirsch- De Mesmaeker, A. *Dalton Trans.* **2004**, 668−676.
(23) Lin, C.-T.; Böttcher, W.; Chou, M.; Creutz, C.; Sutin, N. *J. Am. Chem. Soc.* **1976**, *98*, 6536−6544.
(24) Staniewicz, R. J.; Sympson, R. F.; Hendricker, D. G. *Inorg. Chem.* **1977**, *16*, 2166−2171.
(25) Juris, A.; Balzani, V.; Barigelletti, F.; Campagna, S.; Belser, P.; Vonzelewsky, A. *Coord. Chem. Rev.* **1988**, *84*, 85−277.
(26) Nakamaru, K. *Bull. Chem. Soc. Jpn.* **1982**, *55*, 2697−2705.

Table 3. Emission Data for the Ruthenium(II) Complexes[a]

complex	acetonitrile						water					
	λ_{max}/nm	τ_{air}/ns	τ_{Ar}/ns	$\phi_{Ar}/10^{-3}$	$k_{r(Ar)}/10^3\,s^{-1}$	$k_{nr(Ar)}/10^5\,s^{-1}$	λ_{max}/nm	τ_{air}/ns	τ_{Ar}/ns	$\phi_{Ar}/10^{-3}$	$k_{r(Ar)}/10^3\,s^{-1}$	$k_{nr(Ar)}/10^5\,s^{-1}$
$[Ru(phen)_3]^{2+}$ [23,25,26]	604		460	28	61	21.1	604		920	58	63	10.2
$[Ru(phen)_2(HAT)]^{2+}$	696	371	776	43	55	12.3	732	108	137	7	51	72.5
$[Ru(phen)_2(PHEHAT)]^{2+}$	662	191	262	26	99	37.2						
$[Ru(phen)_2(HATPHE)]^{2+}$	692	366	666	27	41	14.6	730	122	130	7	54	76.4

[a] Complex concentration: 2 × 10^{-5} mol/L. Temperature: 298 K. The emission was corrected for the phototube response. The luminescence decays under pulsed excitation correspond strictly to single exponentials. The experimental errors for the lifetimes are estimated to ±3%. The luminescence quantum yields (ϕ) (approximate error <20%) were determined by comparison with the values for $[Ru(phen)_2(HAT)]^{2+}$ ($\phi_{air} = 17 \times 10^{-3}$). $k_r = \Phi \times 1/\tau$; $k_{nr} = 1/\tau - k_r$.

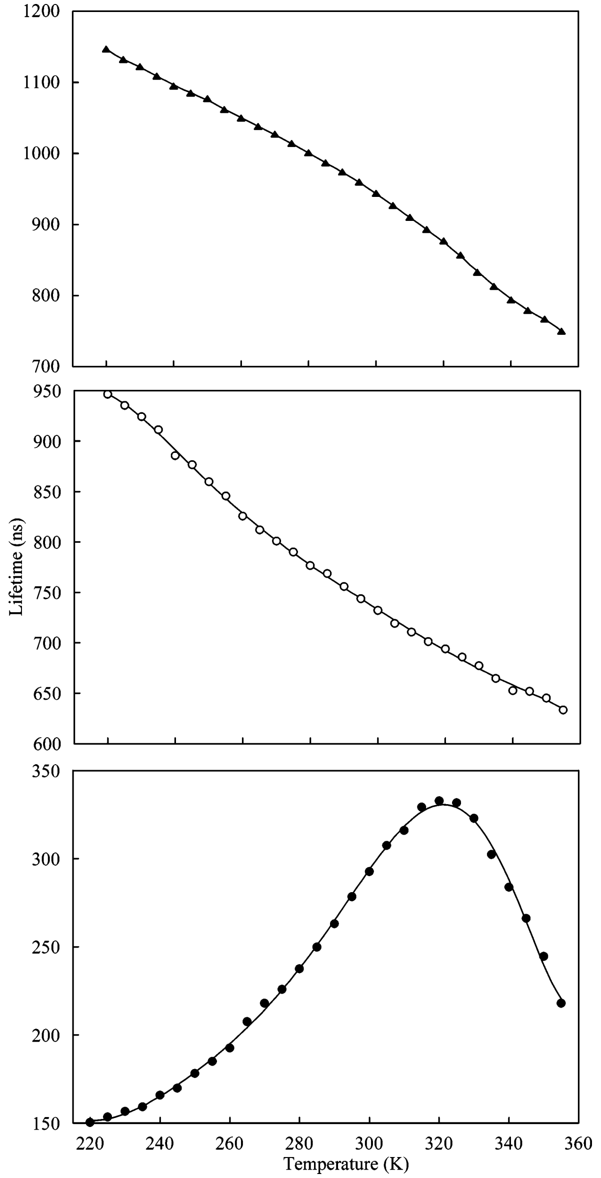

Figure 1. Luminescence lifetimes measured under pulsed laser conditions as a function of temperature for $[Ru(phen)_2(HAT)]^{2+}$ (▲) (at 690 nm), $[Ru(phen)_2(HATPHE)]^{2+}$ (○) (at 690 nm), and $[Ru(phen)_2(PHEHAT)]^{2+}$ (●) (at 660 nm) in butyronitrile.

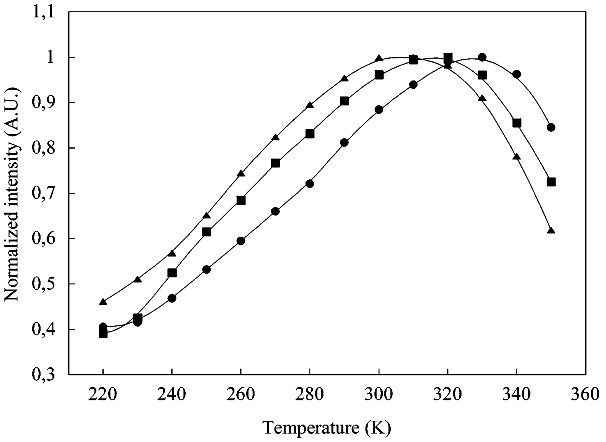

Figure 2. Normalized integrated steady-state emission intensity for $[Ru(phen)_2(PHEHAT)]^{2+}$ in butyronitrile (▲), propionitrile (■), and acetonitrile (●).

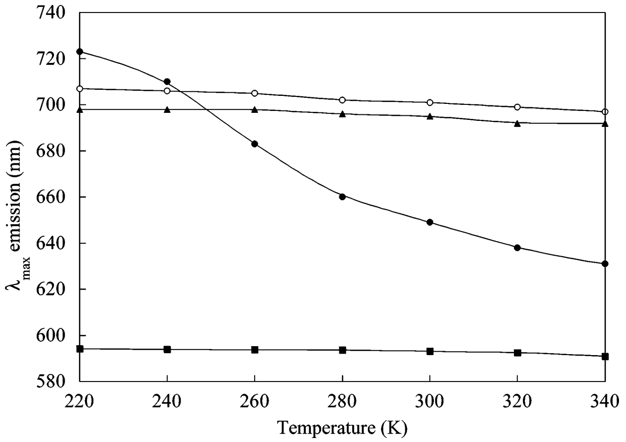

Figure 3. λ_{max} of emission for $[Ru(phen)_2(HAT)]^{2+}$ (▲), $[Ru(phen)_2(HATPHE)]^{2+}$ (○), $[Ru(phen)_2(PHEHAT)]^{2+}$ (●), and $[Ru(phen)_3]^{2+}$ (■) in butyronitrile as a function of temperature.

Table 4. Luminescence Lifetimes (τ) of $[Ru(phen)_2((PHEHAT)]^{2+}$ [a]

$\lambda_{detection}$/nm	τ(291 K)/ns	τ(319 K)/ns
630	407	198
725	348	281

[a] τ measured by SPC at 291 K (left of the maximum of the curve in Figure 1) and at 319 K (right of the maximum of the curve in Figure 1) and obtained from a single-exponential analysis of the emission decay. Error: ±10%.

$[Ru(phen)_3]^{2+}$, and the other in the lower temperature domain, which luminesces in the same wavelength region as the HAT and HATPHE complexes. To test the different contributions of different luminophores as a function of temperature in liquid butyronitrile, the luminescence decays have been analyzed by SPC for the PHEHAT complex at two different temperatures (291 and 319 K) and two different wavelengths of detection (630 and 725 nm) (Table 4).

The luminescence decays do not fit perfectly well to single exponentials. The treatment of the data according to biexponential decays gives excellent fittings but with two rather

Table 5. Emission Maxima for the Ruthenium(II) Complexes at 77 K

complex	λ_{max}/nm [MeOH−EtOH (4:1)]
$[Ru(phen)_3]^{2+}$ [26]	566
$[Ru(phen)_2(PHEHAT)]^{2+}$	598
$[Ru(phen)_2(HATPHE)]^{2+}$	663
$[Ru(phen)_2(HAT)]^{2+}$	650
$[Ru(bpy)_2(HAT)]^{2+}$ [21]	660

close lifetime values with one which contributes only for 1−2%. The values obtained from this treatment are thus not reliable (the lifetimes should differ by at least a factor of 2). Therefore, the lifetimes given in Table 4 correspond to values obtained from a single-exponential treatment with χ^2 extending from 1.2 to 1.7. These data show that the lifetimes decrease from 291 to 319 K, due to the crossing to the ^{3}MC, and this more at 630 nm than at 725 nm.

The λ_{max} values of emission were also measured in a solvent matrix at 77 K (Table 5).

It is noted that as expected for a rigid matrix, the maxima are blue shifted. The values for the HATPHE and HAT complexes are similar. However, whereas, at 220 K (Figure 3) in liquid butyronitrile, the emission maxima of the HAT, HATPHE, and PHEHAT complexes are similar but different from $[Ru(phen)_3]^{2+}$, the situation looks different at 77 K in a matrix MeOH−EtOH. Indeed, under those conditions, the λ_{max} of $[Ru(phen)_2(PHEHAT)]^{2+}$ is no longer similar to that of the HAT and HATPHE complexes but has approached the value for $[Ru(phen)_3]^{2+}$. These data indicate that the emitter of the PHEHAT compound is changing not only with temperature but also when the phase is liquid or solid.

Discussion

Synthesis. To prepare $[Ru(phen)_2(HATPHE)]^{2+}$ (**1**), it is necessary to synthesize the HATPHE ligand on the already chelated Ru(II) ion, from a precursor complex, as it was the case for $[Ru(phen)_2(PHEHAT)]^{2+}$. As the free ligand is quite insoluble in the usual organic solvents, this strategy solves this problem and moreover it allows the preparation of the mononuclear complex at the desired chelation site of the ligand. Thus, **1** is formed from $[Ru(phen)_2Cl_2]$, which reacts with 9,10-diamino-1,4,5,8-tetraazaphenanthrene (diamino-TAP). The obtained precursor complex ($[Ru(phen)_2(diamino\text{-}TAP)]^{2+}$) is condensed with the 1,10-phenanthroline-5,6-dione (phendione) to produce $[Ru(phen)_2(HATPHE)]^{2+}$, which is characterized by NMR spectroscopy and ES-MS analysis.

Spectroscopic and Redox Properties of $[Ru(phen)_2(HATPHE)]^{2+}$. The spectroscopic data show clearly that the HATPHE complex **1** exhibits spectroscopic behaviors quite similar to those of $[Ru(phen)_2(HAT)]^{2+}$. This is clearly concluded by comparing (i) the wavelength of the most bathochromic transition in the MLCT absorption band (i.e. the shoulders) for both complexes, which are quasi identical in water and MeCN, and (ii) the λ_{max} of emission. It is also noted that **1** emits in water like the HAT complex, thus behaving completely differently from $[Ru(phen)_2(PHEHAT)]^{2+}$. Even the values of the deactivation rate constants (k_r and k_{nr}) and the emission lifetimes of the ^{3}MLCT states are rather close for **1** and $[Ru(phen)_2(HAT)]^{2+}$. These similarities suggest that the chromophore and luminophore in **1** would behave like those of a ^{3}MLCT state where the excited electron would be localized on the HAT part of the HATPHE ligand.

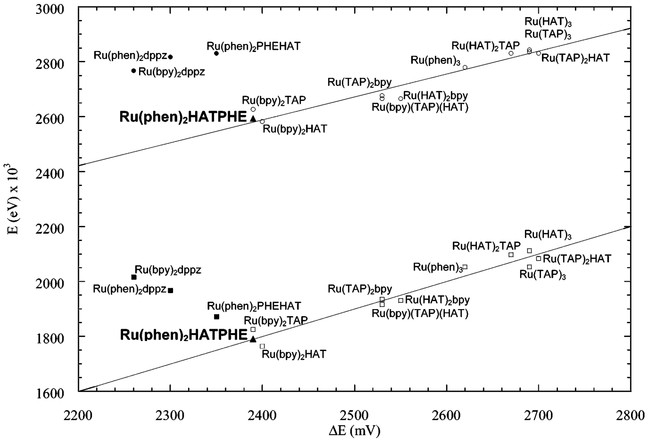

Figure 4. Spectroelectrochemical correlation for a few complexes in absorption (○) and in emission (□).

On the other hand, a consideration of the electrochemical data in reduction for the free ligands HAT and HATPHE and the corresponding complexes (Table 1) indicates that these two ligands behave differently by complexation with the Ru(II) ion. First, the LUMO π^* orbital of the free ligand HATPHE ($E_{red} = -1.10$ V/SCE) is more stabilized than the LUMO orbital of the free ligand HAT ($E_{red} = -1.33$ V/SCE). This is of course expected since HATPHE is a heptacycle and thus has a more extended aromaticity than HAT which has 4 cycles. Next, after complexation of the HAT with the Ru, the LUMO π^* orbital centered on the HAT in the corresponding complex is stabilized by 0.47 V ($E_{red} = -0.86$ V/SCE) whereas, after complexation of the HATPHE ligand, the LUMO π^* orbital centered on the HATPHE in the corresponding complex is stabilized only by 0.27 V ($E_{red} = -0.83$ V/SCE). If it is assumed that the σ-donating power is more or less similar for both ligands (HAT and HATPHE), this different orbital stabilization would mean that the back-bonding effect in the Ru−HATPHE complex is more important than in the Ru−HAT complex. This conclusion seems reasonable, since the HATPHE ligand has a more extended aromaticity than the HAT ligand. From Table 1 it is also concluded that the energy level of the HOMO dπ orbitals of $[Ru(phen)_2(HAT)]^{2+}$ and $[Ru(phen)_2(HATPHE)]^{2+}$ should have a similar energy since the oxidation potentials are similar.

Figure 4 shows that the electrochemical and spectroscopic data in absorption and emission for both HAT and HATPHE complexes fall very well on the spectroelectrochemical correlation line found for most of the Ru complexes. Such a linear correlation between the energy of the transition in absorption or in emission and the difference between the first reduction and the first oxidation potentials does exist indeed when the molecular orbitals involved in the electrochemical process and those involved in the electronic transition are the same.[27] The Ru−HATPHE complex although based on an extended ligand behaves thus quite normally like most of the other complexes.

In contrast, the PHEHAT complex does not behave "normally" (Figure 4) since the spectroscopic and electrochemical data for $[Ru(phen)_2(PHEHAT)]^{2+}$ do not fall on the spectroelectrochemical correlation.

This can be explained by the following. For the absorption, the properties of the chromophore look like those of a Ru−phen MLCT transition in $[Ru(phen)_3]^{2+}$ (Table 2). In electrochemistry, the complex behaves also like $[Ru(phen)_3]^{2+}$, at least for the oxidation (thus a dπ level similar to that of $[Ru(phen)_3]^{2+}$) (Table 1). However, this is not the case for the reduction (thus, π^* level different from that of $[Ru(phen)_3]^{2+}$) (Table 1). Therefore, the data cannot fall on the correlation straight line for the absorption. Concerning the emission, the properties of the luminophore in the Ru−PHEHAT complex are between those of $[Ru(phen)_3]^{2+}$ and $[Ru(phen)_2(HAT)]^{2+}$ (Table 3). In electrochemistry, the reduction potential is also between the reduction potential values of these two complexes, but the oxidation potential is close to that of $[Ru(phen)_3]^{2+}$ (Table 1). Therefore, the emission data are not on the spectroelectrochemical correlation line either.

As usually mentioned, such an absence of correlation is obviously due to the fact that the orbitals involved in spectroscopy are not the same as those involved in electrochemistry. Indeed as developed below, more than one transient species following the absorption of light can be detected for the PHEHAT but not for the HATPHE complex.

Nature of the Excited States in the PHEHAT and HATPHE Complexes. By measurement of the emission lifetimes or emission intensities as a function of temperature, information concerning the transient species that participate in the processes of deactivation of the excited state can be obtained. Generally for the Ru(II) complexes, the emission lifetime increases when the temperature decreases. This is attributed to the fact that the thermal activation from the luminescent ^{3}MLCT state toward the nonluminescent ^{3}MC state decreases at lower temperatures so that the result is an increase of the emission lifetime of the ^{3}MLCT state. As shown in Figure 1, this is indeed the case for $[Ru(phen)_2(HAT)]^{2+}$ and $[Ru(phen)_2(HATPHE)]^{2+}$ in butyronitrile.

Moreover for these two compounds, as shown in Figure 3, the λ_{max} of emission remains quasi the same in the whole investigated temperature domain. This indicates that the emitting species does not change with temperature (emission around 700 nm) and corresponds, for the HAT complex, to the ^{3}MLCT state centered on the HAT ligand and, for the HATPHE complex, to a ^{3}MLCT state where the electron would be mainly localized on the HAT part of the HATPHE ligand. For these two complexes, in a rigid matrix at 77 K, the λ_{max} of emission shifts hypsochromically (Table 5), as it is usually observed in the absence of relaxation of the solvent. Under this condition, the emission maxima are also similar for the HAT and HATPHE complexes. In conclusion, for these two compounds, whose spectroscopic data fall on the spectroelectrochemical correlation line, only one excited ^{3}MLCT state centered on the HAT motif is responsible for the emission.

In contrast, as outlined below, this is not the case for $[Ru(phen)_2(PHEHAT)]^{2+}$ whose spectroelectrochemical data fall outside the correlation. As shown in Figures 1 and 2, the lifetimes and intensities of emission in butyronitrile as a function of temperature exhibit a maximum as found for $[Ru(bpy/phen)_2(dppz)]^{2+}$.[6,9,10]

The model, which has been proposed in the literature[6] to explain the presence of such a maximum for $[Ru(bpy)_2(dppz)]^{2+}$, could be applied to the case of the PHEHAT complex. Thus, as outlined in the Introduction, instead of continuing increasing at low temperatures, the luminescence lifetime starts decreasing because a dark (D) state would get populated and would participate to the deactivation. As the same behavior is observed with the PHEHAT complex, it could also be concluded that a D state participates at low temperature. Moreover in agreement with this model discussed in the literature for the dppz complex, Figure 2 shows that this maximum found by plotting the emission lifetime or intensity versus the temperature shifts to higher temperatures from butyronitrile to propionitrile to acetonitrile. Thus, if the same type of explanation is extended to the PHEHAT complex, this shift of maximum would have the following origin. The D state populated at low temperature would correspond to a species slightly different from the bright (B) excited ^{3}MLCT state. In the B state, the electron transferred from the Ru to the ligand would be localized on the phen part of the PHEHAT ligand, whereas, in the D state, the charges would be more separated; thus, the electron would be localized further from the metal center. Therefore, as this D state would have a higher dipole moment than the B state, it would be more stabilized from butyronitrile to propionitrile to acetonitrile. The luminescence behavior of the PHEHAT complex fits thus well with the model proposed for the dppz complex. Moreover, if the PHEHAT and dppz results are compared, it may be concluded that the temperature for the appearance of the maximum is higher for the PHEHAT than for the dppz compound in the same solvent.[9] This would mean that the D state of the PHEHAT compound would be more stabilized (thus would have a higher dipole moment) than that of the dppz complex, which seems reasonable.

There is however an important difference of behavior between the PHEHAT and dppz complexes. Indeed Figure 3 shows that the λ_{max} of emission exhibits an important shift with temperature. For the dppz complexes, there is no indication of such a shift in ref 9, whereas, in ref 10, the authors mention a very slight shift. Thus, as clearly indicated by the shift for the PHEHAT complex, at least two luminophores should be present, one at higher temperature with characteristics (emission around 630 nm) close to those of $[Ru(phen)_3]^{2+}$ and one at lower temperature with characteristics (emission around 720−725 nm) close to those of the HAT or HATPHE complex.

---

[27] Paul Rillema, D.; Allen, G.; Meyer, T. J.; Conrad, D. V. *Inorg. Chem.* **1983**, *22*, 1617−1622.

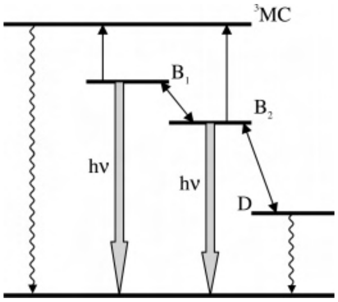

Figure 5. Schematic representation of the energy levels in $[Ru(phen)_2(PHEHAT)]^{2+}$.

It is thus concluded that, in the case of $[Ru(phen)_2(PHEHAT)]^{2+}$, there would be two B states: one populated at higher temperature (B_1, Figure 5), which would correspond to a ^{3}MLCT state with the electron more localized on the phen part of PHEHAT, and one at lower energy (B_2), populated at lower temperature, which would correspond to a ^{3}MLCT state with the electron localized on the HAT part of the PHEHAT. This lower energy state B_2 would have a higher dipole moment than B_1 with the phen-like characteristics and, in the low temperature domain, a shorter luminescence lifetime. Indeed the lifetime, measured by SPC (Table 4), is slightly shorter at 725 nm (wavelength at which the contribution of B_1 would decrease in favor of B_2) than at 630 nm (wavelength at which the contribution of the higher energy state, B_1, would be important). Moreover at 630 nm the lifetime strongly decreases (by 200 ns) from 291 to 319 K, because of an efficient crossing of B_1 to the ^{3}MC state. In contrast, at 725 nm the decrease of the lifetime from 291 to 319 K is less important (decrease of 60 ns) because the crossing of B_2 to the ^{3}MC state would be less efficient than for B_1.

It should also be stressed that the lower energy state B_2 would be reached by solvent relaxation around the PHEHAT ligand in the excited complex. Indeed if relaxation cannot take place (case at 77 K, Table 5), only the higher energy ^{3}MLCT state (B_1) remains populated, as indicated by the λ_{max} of emission in the solvent matrix (598 nm), which is far from that of the HAT and HATPHE complexes (Table 5) but closer to the λ_{max} of emission of $[Ru(phen)_3]^{2+}$.

Because of the existence of these two types of emitting ^{3}MLCT states, differently populated as a function of temperature, the presence of a D state is maybe no longer necessary to explain the maximum in the curves obtained by plotting the lifetimes or emission intensities as a function of temperature. As developed below, the participation of this dark state with a much shorter lifetime has however to be considered. First at 319 K (higher temperature domain, Table 4), the emission lifetime is longer (281 ns) at 725 nm than at 630 nm (198 ns). This slightly longer lifetime at 725 nm, as mentioned above, would be attributed to an increased contribution of B_2 lower in energy than B_1 and thus less activated to the ^{3}MC state than B_1. Therefore, at lower temperature, such as 220 K, the measured lifetime (Figure 1) should be longer than 281 ns since the crossing for *both* B_1 and B_2 to the ^{3}MC state should decrease. However, this is not the case since, at 220 K, the measured lifetime is only 150 ns. Therefore, a third state such as a D state should be responsible for the important decrease of lifetime from ~320 to 220 K (Figure 1).

In alcohol (propanol) (see Supporting Information), a maximum is also observed in the plot of the emission intensity versus temperature. However, the emission intensity is too weak to detect differences with the emission wavelength. The maximum is shifted to higher temperatures as compared to butyronitrile and propionitrile. This indicates, as demonstrated for the dppz complex,[10] that, in alcohol, the lower energy state of the PHEHAT complex would be also more stabilized due to H-bonding and under these conditions a nonluminescent H-bonded state could contribute to the deactivation in the low-temperature domain (relative to the temperature at the maximum). In water the complex does not emit at all even at higher temperatures. In connection with the possibility of H-bond formation, it is interesting to note that the HAT and HATPHE complexes as mentioned above luminesce in water with a normal quantum yield of emission. This difference of behavior in water between the HAT/HATPHE complexes on one hand and the PHEHAT compound on the other hand could be due to a slightly higher basicity of the HAT motif in the PHEHAT complex as compared to the basicity of the HAT/HATPHE in the two other complexes. Indeed when the HAT part is chelated to a Ru center, it would be more deficient in electrons than the HAT motif with a free chelation site (case of the PHEHAT complex), which therefore would be more basic and thus prone to formation of H-bonds.

Conclusion

The results of this work show that the site of chelation on the PHEHAT/HATPHE ligand has a dramatic influence on the photophysical and electrochemical properties of the complex. Moreover, the comparison between the HATPHE and PHEHAT complexes sheds also some light on the peculiar behavior of the PHEHAT compound, which has important similarities with the dppz complexes. However, in contrast to these latter, two distinct emitting states can clearly be detected for the PHEHAT complex and are differently populated depending on the temperature.

Acknowledgment. The authors thank the ARC (Action de Recherche Concertée, 2002−2007) and the FNRS-Belgium (Fonds National pour la Recherche Scientifique) for their financial support. They are grateful to the Laboratoire de Spectrométrie de Masse Bio-Organique (University Louis Pasteur, Strasbourg, France) for the ES mass spectrometry measurements.

Supporting Information Available: A figure for the integrated steady-state emission intensity of $[Ru(phen)_2(PHEHAT)]^{2+}$ in propanol as a function of temperature. This material is available free of charge via the Internet at http://pubs.acs.org.

IC051306F